



Heriot-Watt University

Heriot-Watt University
Research Gateway

Mid-infrared volume phase gratings manufactured using ultrafast laser inscription

MacLachlan, David Guillaume; Thomson, Robert R; Cunningham, Colin R; Lee, David

Published in:
Optical Materials Express

DOI:
[10.1364/OME.3.001616](https://doi.org/10.1364/OME.3.001616)

Publication date:
2013

[Link to publication in Heriot-Watt Research Gateway](#)

Citation for published version (APA):
MacLachlan, D. G., Thomson, R. R., Cunningham, C. R., & Lee, D. (2013). Mid-infrared volume phase gratings manufactured using ultrafast laser inscription. *Optical Materials Express*, 3(10), 1616-1624.
10.1364/OME.3.001616



General rights

Copyright and moral rights for the publications made accessible in the public portal are retained by the authors and/or other copyright owners and it is a condition of accessing publications that users recognise and abide by the legal requirements associated with these rights.

If you believe that this document breaches copyright please contact us providing details, and we will remove access to the work immediately and investigate your claim.

Mid-Infrared Volume Phase Gratings Manufactured using Ultrafast Laser Inscription

David G. MacLachlan,^{1,*} Robert R. Thomson,¹ Colin R. Cunningham,² and David Lee²

¹Scottish Universities Physics Alliance (SUPA), Institute of Photonics and Quantum Sciences, Heriot-Watt University, Edinburgh, EH14 4AS, U.K.

²Science and Technology Facilities Council, UK Astronomy Technology Centre, Royal Observatory, Blackford Hill, Edinburgh, EH9 3HJ, U.K.
dgm4@hw.ac.uk

Abstract: We report on the ultrafast laser inscription (ULI) of volume phase gratings inside gallium lanthanum sulphide (GLS) chalcogenide glass substrates. The effect of laser pulse energy and grating thickness on the dispersive properties of the gratings is investigated, with the aim of improving the performance of the gratings in the mid-infrared. The grating with the optimum performance in the mid-infrared exhibited a 1st order absolute diffraction efficiency of 61% at 1300 nm and 24% at 2640 nm. Based on the work reported here, we conclude that ULI is promising for the fabrication of mid-infrared volume phase gratings, with potential applications including astronomical instrumentation and remote sensing.

©2013 Optical Society of America

OCIS codes: (050.1950) Diffraction gratings; (050.7330) Volume gratings; (140.3390) Laser materials processing; (230.1950) Diffraction gratings.

References

1. K. M. Davis, K. Miura, N. Sugimoto, and K. Hirao, "Writing waveguides in glass with a femtosecond laser," *Opt. Lett.* **21**(21), 1729–1731 (1996).
2. Y. Kondo, T. Suzuki, H. Inouye, K. Miura, T. Mitsuyu, and K. Hirao, "Three-dimensional microscopic crystallization in photosensitive glass by femtosecond laser pulses at nonresonant wavelength," *Jpn. J. Appl. Phys.* **37**(Part 2, No. 1A/B), L94–L96 (1998).
3. A. Marcinkevičius, S. Juodkakis, M. Watanabe, M. Miwa, S. Matsuo, H. Misawa, and J. Nishii, "Femtosecond Laser-assisted three-dimensional microfabrication in silica," *Opt. Lett.* **26**(5), 277–279 (2001).
4. R. R. Thomson, T. A. Birks, S. G. Leon-Saval, A. K. Kar, and J. Bland-Hawthorn, "Ultrafast laser inscription of an integrated photonic lantern," *Opt. Express* **19**(6), 5698–5705 (2011).
5. A. Ródenas, G. Martin, B. Arezki, N. Psaila, G. Jose, A. Jha, L. Labadie, P. Kern, A. Kar, and R. Thomson, "Three-dimensional mid-infrared photonic circuits in chalcogenide glass," *Opt. Lett.* **37**(3), 392–394 (2012).
6. R. R. Thomson, R. J. Harris, T. A. Birks, G. Brown, J. Allington-Smith, and J. Bland-Hawthorn, "Ultrafast laser inscription of a 121-waveguide fan-out for astrophotonics," *Opt. Lett.* **37**(12), 2331–2333 (2012).
7. Y. Cheng, H. L. Tsai, K. Sugioka, and K. Midorikawa, "Fabrication of 3D microoptical lenses in photosensitive glass using femtosecond laser micromachining," *Appl. Phys. A: Mater.* **85**(1), 11–14 (2006).
8. Y. Bellouard, A. Said, and P. Bado, "Integrating optics and micro-mechanics in a single substrate: a step toward monolithic integration in fused silica," *Opt. Express* **13**(17), 6635–6644 (2005).
9. N. Bellini, K. C. Vishnubhatla, F. Bragheri, L. Ferrara, P. Minzioni, R. Ramponi, I. Cristiani, and R. Osellame, "Femtosecond laser fabricated monolithic chip for optical trapping and stretching of single cells," *Opt. Express* **18**(5), 4679–4688 (2010).
10. G. D. Marshall, A. Politi, J. C. F. Matthews, P. Dekker, M. Ams, M. J. Withford, and J. L. O'Brien, "Laser written waveguide photonic quantum circuits," *Opt. Express* **17**(15), 12546–12554 (2009).
11. N. Jovanovic, P. G. Tuthill, B. Norris, S. Gross, P. Stewart, N. Charles, S. Lacour, M. Ams, J. S. Lawrence, A. Lehmann, C. Niel, J. G. Robertson, G. D. Marshall, M. Ireland, A. Fuerbach, and M. J. Withford, "Starlight demonstration of the Dragonfly instrument: an integrated photonic pupil-remapping interferometer for high-contrast imaging," *Mon. Not. R. Astron. Soc.* **427**(1), 806–815 (2012).
12. S. Minardi, F. Dreisow, M. Gräfe, S. Nolte, and T. Pertsch, "Three-dimensional photonic component for multichannel coherence measurements," *Opt. Lett.* **37**(15), 3030–3032 (2012).
13. R. R. Thomson, N. D. Psaila, S. J. Beecher, and A. K. Kar, "Ultrafast laser inscription of a high-gain Er-doped bismuthate glass waveguide amplifier," *Opt. Express* **18**(12), 13212–13219 (2010).
14. S. Barden, J. Arns, W. Colburn, and J. Williams, "Volume-phase holographic gratings and the efficiency of three simple volume-phase holographic gratings," *Publ. Astron. Soc. Pac.* **112**(772), 809–820 (2000).

15. A. Y. Naumov, C. Przygodzki, X. Zhu, and P. B. Corkum, "Microstructuring with femtosecond laser inside silica glasses," *Lasers and Electro-Optics, CLEO* **99**, 356–357 (1999).
16. L. Sudrie, M. Franco, B. Prade, and A. Mysyrowicz, "Writing of permanent birefringent microlayers in bulk fused silica with femtosecond laser pulses," *Opt. Commun.* **171**(4-6), 279–284 (1999).
17. K. Yamada, W. Watanabe, K. Kintaka, J. Nishii, and K. Itoh, "Fabrication of volume grating induced in silica glass by femtosecond laser," *Proc. SPIE* **5063**, 474–477 (2003).
18. R. Martinez-Vazquez, R. Osellame, G. Cerullo, R. Ramponi, and O. Svelto, "Fabrication of photonic devices in nanostructured glasses by femtosecond laser pulses," *Opt. Express* **15**(20), 12628–12635 (2007).
19. F. He, H. Sun, M. Huang, J. Xu, Y. Liao, Z. Zhou, Y. Cheng, Z. Xu, K. Sugioka, and K. Midorikawa, "Rapid fabrication of optical volume gratings in Foturan glass by femtosecond laser micromachining," *Appl. Phys. A. Mater.* **97**(4), 853–857 (2009).
20. Q. Z. Zhao, J. R. Qiu, X. W. Jiang, C. J. Zhao, and C. S. Zhu, "Fabrication of internal diffraction gratings in calcium fluoride crystals by a focused femtosecond laser," *Opt. Express* **12**(5), 742–746 (2004).
21. C. Voigtländer, D. Richter, J. Thomas, A. Tünnermann, and S. Nolte, "Inscription of high contrast volume Bragg gratings in fused silica with femtosecond laser pulses," *Appl. Phys. A. Mater.* **102**(1), 35–38 (2011).
22. M. A. Hughes, W. Yang, and D. W. Hewak, "Spectral broadening in femtosecond laser written waveguides in chalcogenide glass," *J. Opt. Soc. Am. B* **26**(7), 1370–1378 (2009).
23. D. Lee, R. R. Thomson, and C. R. Cunningham, "Performance of volume phase gratings manufactured using ultrafast laser inscription," *Proc. SPIE* **8450**, 84502X1–84502X-9 (2012).

1. Introduction

Ultrafast laser inscription (ULI) is a rapidly maturing fabrication process that facilitates the direct-laser writing of three-dimensional structures inside dielectric materials. To perform ULI, sub-bandgap ultrashort laser pulses are focused inside the substrate. Nonlinear absorption processes, such as multiphoton absorption, tunnelling ionization and avalanche ionization, deposit optical energy in the focal region. This deposition of energy can induce a localised structural modification, which can manifest itself in a variety of ways e.g. refractive index change [1] or chemical etch-rate modification [2, 3]. By translating the material through the laser focus, the ULI induced refractive index modulation can be used to fabricate three dimensional optical waveguide structures [4–6], while the ULI induced chemical etch-rate modification can be used to fabricate micro-optic [7], micro-mechanic [8] and micro-fluidic [9] structures. The applications of such a unique and flexible fabrication technology are vast, and those currently under investigation include (but are not limited to) quantum-optics [10], astrophotonics [4–6, 11, 12], biophotonics [9], and telecommunications [13].

In this paper we report on the ULI fabrication of volume phase gratings in gallium lanthanum sulphide (GLS) chalcogenide glass substrates, primarily with a view towards future mid-IR applications in astronomy, space-science and remote-sensing. The motivation behind this work is three-fold. Firstly, commercial volume phase holographic gratings (VPHGs) are most commonly fabricated in dichromated gelatine [14], which restricts the long wavelength operation to below ~2200 nm. Secondly, gelatine VPHGs are fabricated by exposing the material to an interference pattern – this restricts the size and form of the refractive index structure that can be realised. Thirdly, traditional VPHGs are extremely fragile. The application of ULI could address each of these drawbacks. For example, ULI may facilitate the fabrication of volume phase gratings in mid-IR transmitting materials, such as the GLS glass used in this work. Furthermore, since ULI is a direct-write technology there is no need for an interferometer, thus it may enable the fabrication of large volume phase gratings with variable line spacing, blazed profiles, or curved lines. Lastly, in contrast to traditional gelatine VPHGs, ULI fabricated volume phase gratings are extremely robust since the grating is fabricated at depth inside a single robust glass substrate.

It is important to state that there have been many previous studies aimed at exploring the ULI manufacture of diffraction gratings. Early studies used fused silica substrates [15, 16] and achieved a peak efficiency of 20% @ 633nm [16]. Later development of fused silica gratings [17] resulted in diffraction efficiencies of 75% and 59% being measured for TE and TM polarized 633 nm light respectively. From these measurements, a refractive index modulation of 0.002 – 0.01 was calculated via Kogelnik's coupled wave theory [14]. Gratings have also been manufactured in Schott filter glass OG530 [18] and demonstrated a large

refractive index modulation of 0.018, and a peak diffraction efficiency of 37% @ 633nm. Gratings have also been manufactured in Foturan photosensitive glass [19] with peak efficiency of 56% @ 633nm, but the refractive index modulation was not mentioned. Gratings with the potential to operate in the mid-IR have been manufactured in CaF₂ [20], but the low refractive index modulation of 0.00036 resulted in gratings with a low diffraction efficiency of 8.5% @ 633nm. It is also worth highlighting recent work [21], which demonstrated the ULI fabrication of a high efficiency volume Bragg-grating in fused silica using a phase mask base technique. These previous studies, and others, clearly demonstrate that diffraction gratings can be manufactured using ULI in a wide variety of materials and high diffraction efficiency can be obtained. In this work, we explore the potential of using ULI to fabricate efficient volume phase dispersive transmission gratings for the mid-IR, beyond 2200 nm.

2. Volume grating fabrication details

All gratings were fabricated in GLS chalcogenide glass ($n \sim 2.4$) using ULI. GLS was chosen for two reasons: its ability to produce a relatively high refractive index modulation [5] and its good transmittance over the wavelength range 500 nm \rightarrow 10 μ m, with its potential application to near-IR and mid-IR astronomical spectroscopy. The ULI process was performed using an ultrafast Ytterbium-doped fiber laser system (Fianium HE1060-fs) which produced 430 fs pulses of 1064 nm light at a pulse repetition frequency of 500 kHz. The substrate material was mounted on x-y-z crossed-roller bearing translation stages (Aerotech ANT130) which facilitated the smooth and precise translation of the sample through the laser focus. The gratings were fabricated by circularly polarizing the laser and focusing it inside the substrate using a 0.4 NA lens. The substrate was then repetitively scanned back and forth through the laser focus at a translation velocity of 10 mm.s⁻¹. Each full volume phase grating was fabricated by inscribing 1000 parallel lines of modified material, with a line spacing of 3.0 μ m. The specification of the translation stages indicates that the grating period should be stable to ± 125 nm. Individual grating lines were inscribed by translating the material only once through the laser focus and adjacent lines were inscribed using opposite sample translation directions. The complete grating was constructed by repeating this process a number of times. Each time the process was started at the same position in the glass, except for the depth of the inscription, which was reduced by 2.4 μ m for each additional layer, such the grating is manufactured with deeper modifications inscribed first. A similar process was used to extend the depth of the gratings demonstrated in [18]. The ULI technique can be adapted for the manufacture of reflective volume Bragg-gratings as discussed in [21].

3. Volume grating studies

3.1 Inscription pulse energy study

To investigate the optimum pulse energy for grating inscription, volume phase gratings were fabricated which consisted of 17 layers of index modification, resulting in gratings ~ 41 μ m thick and finishing ~ 150 μ m below the surface. A preliminary investigation (Sample A) was first conducted where gratings were fabricated using pulse energies between 10 nJ and 180 nJ. Based on the 1st order diffraction efficiency of 633 nm light, measured at blaze, this preliminary study indicated that the optimum pulse energy lay between 60 nJ and 90 nJ. Using the results of the preliminary study, 16 gratings were then inscribed using pulse energies between 62 nJ and 92 nJ, in 2 nJ steps (Sample B). Figure 1 shows two pictures of Sample B. The left image clearly shows light diffracted by the 16 gratings. The right image was taken using a shadowgraph. The yellow appearance of the GLS grating is due to the natural color of the substrate material, whereas the dark color of the gratings is related to the amount of diffracted light such that a darker color indicates a more efficient grating at visible wavelengths.

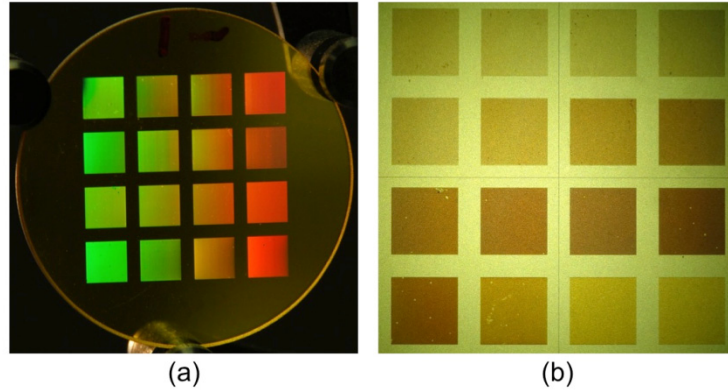


Fig. 1. (a) Digital camera picture of Sample B taken with angled illumination and viewing. (b) Shadowgraph image of Sample B. The orientation in both images is the same. The pulse energy used to fabricate the gratings decreases from left to right for each row and from top to bottom.

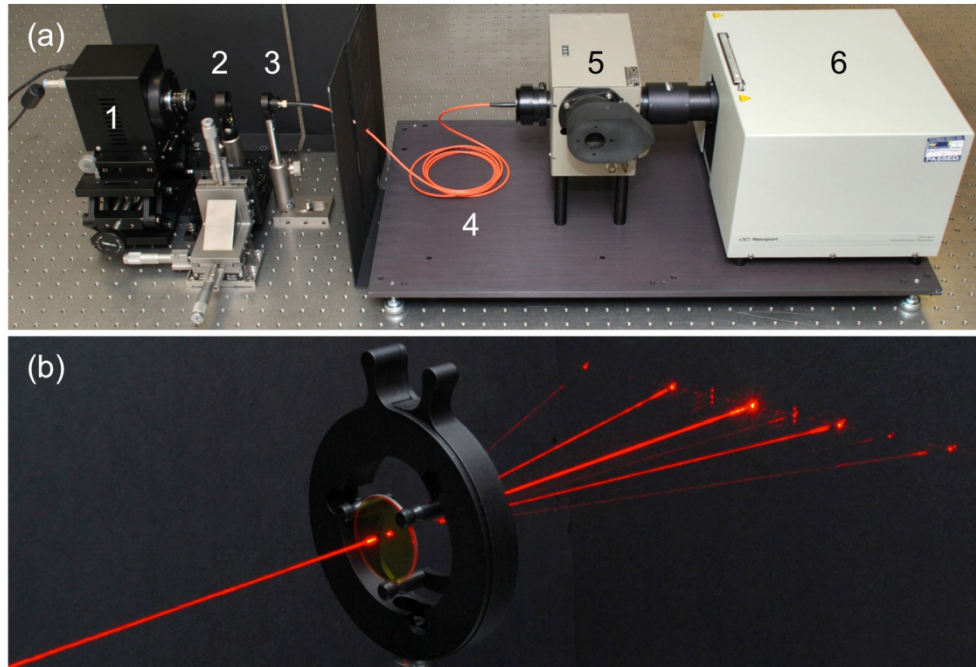


Fig. 2. (a) Digital camera picture of the experimental setup used to measure the broadband efficiency of the gratings. The pieces of equipment shown are the IR camera (1), diffraction grating (2), collimating lens (3), optical fiber (4), monochromator (5) and light source (6). (b) Digital camera picture of one of the GLS gratings illuminated with a 633 nm laser.

The diffraction efficiency of the gratings was measured using the experimental setup shown in Fig. 2(a). The setup consists of a white light source, an order sorting filter, a monochromator, an optical fiber, a collimator lens, the grating under test, and a detector. The light source is intensity stabilised and provides an output with less than 0.5% root mean square ripple. The monochromator operates over the wavelength range 400 – 4000 nm, with the appropriate grating installed, and provides a bandpass of 4 nm to 20 nm depending on the slit selected. An interchangeable order sorting filter is used to block second and third order diffracted wavelengths from the grating in the monochromator. An optical fiber (either a

multimode silica fiber or chalcogenide As_2S_3 infrared fiber from Fibre Photonics, depending on the wavelength range under test) is used to efficiently couple the light from the monochromator to a small collimator lens. The gratings under test are only 3 mm in size, so it was important to test them using a small collimated beam. Thus, the beam size was restricted to 2 mm diameter by an aperture placed at the output of the collimator lens. The intensity of the diffracted beams is measured using either a Hamamatsu silicon photodiode or a Xenics Xeva-2.5-320 infrared camera system to cover the wavelength range 400 – 1000 nm and 1000 – 2600 nm respectively. Both the grating and the detector are mounted on separate rotation and translation stages to provide accurate positioning and alignment during testing.

The image in Fig. 2(b) shows the diffraction pattern produced by a typical grating from Sample A. The image was taken using a long exposure, e.g. 20 seconds, in a darkened room. During the exposure a piece of black card is moved by hand through the laser beam so that the camera captures the position of the beam. At the end of the exposure the card is removed from the scene and a flash is used to expose the image of the grating and mounting hardware.

Figure 3 presents the results of the 633 nm diffraction efficiency measurements for Sample B, measured at blaze to maximise efficiency (where angle of incidence = angle of diffraction = 6 degrees). Figure 3, and all of the subsequent graphs and results present the absolute diffraction efficiency which includes the external transmittance of the substrate material. As shown in Fig. 3, the grating with the highest diffraction efficiency was found to be the one inscribed with 72 nJ laser pulses. For our experimental setup and parameters, this value represents the optimum pulse energy for volume grating fabrication in the GLS material. The precise reasons for this optimum have not been investigated. However, as shown in [22], when using ULI to write structures in GLS glass, the pulse energy not only affects the magnitude of the induced refractive index change, but also its width and profile. We conclude, therefore, that our optimum pulse energy is the one which balances all of these phenomena to maximise the diffraction efficiency. Clearly, the optimum pulse energy could, and indeed would, be expected to vary with other parameters such as translation speed, grating period etc. As discussed extensively in [14], the grating efficiency is a function of the grating thickness, and we expected that mid-IR gratings would require thicker gratings for efficient operation. In the following section we investigate the grating performance as a function of grating thickness.

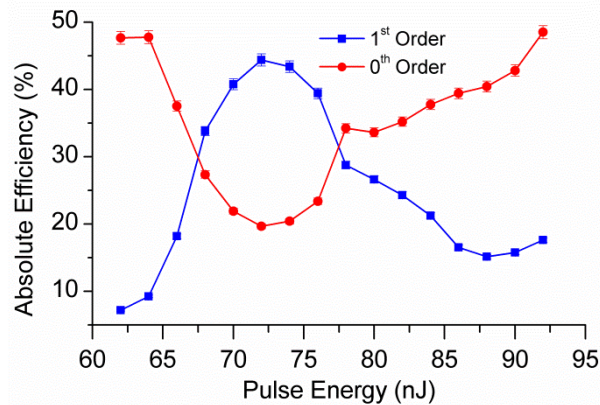


Fig. 3. Plot of absolute diffraction efficiency measured at 633 nm, for 0th and 1st diffraction orders vs. laser pulse energy for Sample B.

3.2 Grating thickness study

Using the optimum pulse energy evaluated from the results of Sample B (72 nJ), a third sample was fabricated, denoted Sample C, containing 4 gratings. Each of these gratings was fabricated using identical parameters, except that the number of layers was either 17, 35, 53 or 71, resulting in grating thicknesses of 41, 84, 127, 170 μm respectively. These gratings were then tested using the experimental setup shown in Fig. 2(a) in order to evaluate the peak 1st order diffraction efficiency as a function of wavelength for each grating. The results of these investigations are shown in Fig. 4 where it can be seen that the thickest grating, fabricated using 71 layers, exhibited the peak efficiency at the longest wavelength, thus indicating the most promise for efficient mid-IR operation. Consequently, the 71 layer grating was further tested using Littrow illumination conditions to determine the diffraction efficiency, for both 0th and 1st orders, as a function of wavelength. The measured efficiency curve is shown in Fig. 5, where it can be seen that the peak efficiency is $61 \pm 2\%$ at 1300 nm. The grating continues to show significant diffraction efficiency of $24 \pm 2\%$ at 2640 nm, the upper wavelength limit of the measurement apparatus.

Of the four Sample C gratings shown in Fig. 4 the one with 53 layers has the highest absolute diffraction efficiency at 65%. This value is consistent with theoretical predictions of grating efficiency made using G Solver grating modelling software and discussed later. The 17 layer grating has low peak efficiency as a result of absorption losses in the GLS substrate material at wavelengths below 650 nm. At wavelengths above 700 nm the GLS substrate transmittance is approximately constant at $\sim 70\%$. The peak efficiency of the gratings with 35 and 71 layers is somewhat lower than the theoretical maximum and this may indicate the presence of a manufacturing tolerance such as misalignment of the grating layers, or a change in the refractive index of the modified region, resulting in lower diffraction efficiency.

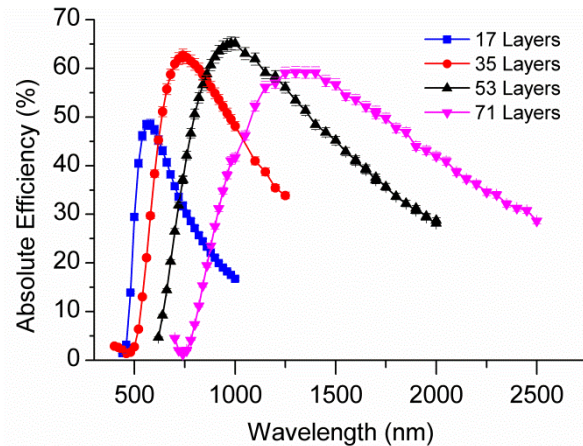


Fig. 4. Plot of absolute diffraction efficiency in 1st order vs. wavelength for Sample C with gratings of different thicknesses.

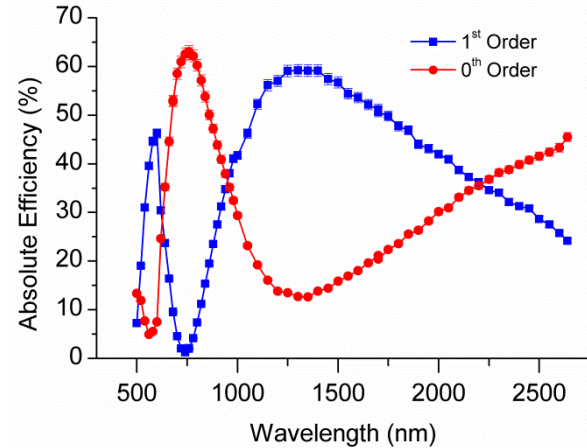


Fig. 5. Plot of absolute diffraction efficiency in 0th and 1st order vs. wavelength for the Sample C grating manufactured with 71 layers.

The blaze angle performance of the 71 layer grating on Sample C was then tested in more detail to determine its diffraction efficiency as a function of angle of incidence. A plot of the 0th and 1st order diffraction efficiency, measured at 1300 nm is shown in Fig. 6. The peak diffraction efficiency occurs at an angle of approximately 12 degrees consistent with the predicted blaze angle. The peak 1st order efficiency of 61% is the absolute efficiency and includes absorption and reflection losses caused by the GLS substrate material. The measured external transmittance of the GLS substrate at 1300 nm is 72%. If the substrate had an efficient anti-reflection coating, we would expect to obtain a peak diffraction efficiency of 85%. Figure 6 also presents the results of theoretical simulations made with GSolver grating modelling software. The parameters used in the GSolver simulations were obtained by first fitting the experimental data by varying the Δn of the simulated grating, and then by varying the depth of the simulated grating. Three different grating profiles were also investigated (binary, sinusoidal and stepped). The measured data is best fit using a 150 μm thick binary grating, where the width of the region of increased index is 0.9 μm and the index modulation is $\Delta n = 0.0075$. We note that the fitted grating thickness is somewhat lower than the expected grating thickness. We suspect that this may be due to a depth dependent variation in the ULI induced Δn – the result of depth dependent spherical aberration imparted on the laser beam.

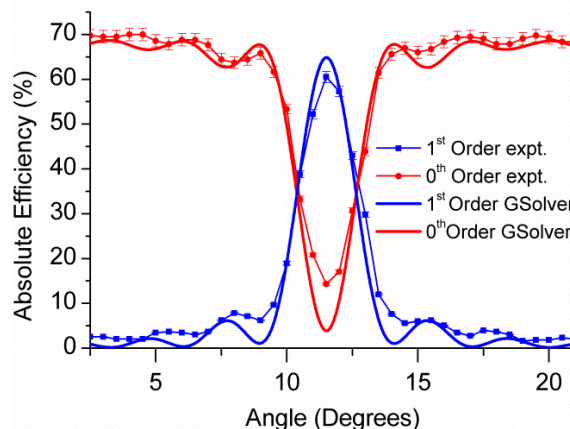


Fig. 6. Plot of absolute diffraction efficiency measured at 1300 nm, for 0th and 1st diffraction orders vs. angle of incidence for the GLS Sample C 71 layer grating. The theoretical GSolver prediction for a binary refractive index profile is also shown.

As seen in Fig. 2(b), the GLS gratings exhibit a stripe of scattered light and ghosts between the main diffraction orders. The amount of scattered light was determined by measuring the total integrated transmittance of the grating and subtracting the known efficiency of the diffraction orders [23]. The total integrated transmittance includes the contribution from all of the diffraction orders, ghosts, and the halo of scattered light. The total integrated transmittance is measured by placing the entrance aperture of the integrating sphere within a few millimetres of the grating, such that most of the output beam is captured. Sample A produced less than 5% integrated scattered light at 633 nm but this is inferred to be < 1% at 2500 nm. The ULI process in GLS performs well, producing highly transparent gratings.

If this grating technology is to be used at mid-IR wavelengths (>2500 nm) it is important to demonstrate that the gratings can survive cooling to cryogenic temperatures and that their performance is unaffected by cooling. To achieve this GLS gratings have been subjected to a number of thermal cycles, from room temperature to 20 K. The diffraction efficiency, measured at room temperature, is unaffected by the thermal cycling. The efficiency at cryogenic temperatures has not yet been characterised but is unlikely to be significantly affected by cooling. The performance of the GLS gratings has been monitored over a period of 18 months and no change in the diffraction efficiency has been detected.

4. Conclusions

This work has demonstrated the capability of ULI to write volume phase diffraction gratings in GLS material and obtain 1st order diffraction efficiency exceeding 61% in the near-IR, and up to 24% at 2640 nm (mid-IR). Simulations indicate that the grating performance is best modeled by a binary refractive index modulation of 0.0075, and not a sinusoidal modulation as in a holographic grating. The robust nature of the ULI grating structures, the ability to manufacture them in a wide range of materials, the ability to create arbitrary grating structures, and their high performance, make them well suited to a variety of applications e.g. hyper-spectral imaging, satellite sensors, small laboratory spectrometers and wavelength-stabilization elements for mid-IR lasers. The excellent performance of the prototype GLS gratings is such that their use in astronomical spectrometers should be considered, particularly at near and mid-IR wavelengths, where GLS provides excellent transmission.

Acknowledgments

The authors acknowledge support from the STFC through RRT's Advanced Fellowship (ST/H005595/1) & the Centre for Instrumentation, OPTICON (EU-FP7 226604), Royal Society (RG110551), Renishaw PLC., Fianium Ltd., ChG Southampton Ltd., Karen McGeachy & Jason Cowan.